

Supporting Information

Two amino-functionalized metal-organic frameworks with different topologies for C₂H₂/C₂H₄ separation

Yue Li,^a Mingming Xu,^a Hongyan Liu,^a Xiaokang Wang,^{*a} Yutong Wang,^a Meng Sun,^a Weidong Fan^{*ab} and Daofeng Sun^{*ab}

^a *School of Materials Science and Engineering, China University of Petroleum (East China), Qingdao, Shandong, 266580, China.*

^b *State Key Laboratory of Heavy Oil Processing, China University of Petroleum (East China), Qingdao, Shandong, 266580, China.*

**Corresponding author E-mail: xiaokangwang0625@163.com, wdfan@upc.edu.cn, dfsun@upc.edu.cn*

Table of Contents

- S1. Materials and instrumentation
- S2. Calculation of isosteric enthalpy of adsorption (Q_{st})
- S3. Calculation of selectivity via ideal adsorption solution theory (IAST)
- S4. Synthesis of Ligands
- S5. Synthesis of MOFs
- S6. Single crystal X-ray Crystallography
- S7. Powder X-ray Diffraction
- S8. $^1\text{H-NMR}$ spectral data
- S9. Thermogravimetric Analysis
- S10. IR spectrum
- S11. SEM images
- S12. Structure diagram of UPC-122
- S13. Adsorption isotherms of UPC-122 at 273 K
- S14. Adsorption sites simulation based on GCMC
- S15. References

1. Materials and instrumentation

The reagents and solvents were commercially available and were used as received without further purification. Infrared (IR) spectroscopy spectra were collected on a Nicolet 330 FTIR Spectrometer within the 4000–400 cm^{-1} region. Thermogravimetric analysis (TGA) was performed on a Mettler Toledo TGA under N_2 flow and heated from room temperature to 900 $^\circ\text{C}$ (at 10 $^\circ\text{C min}^{-1}$). Powder X-ray diffraction measurements were carried out on an analytical X-Pert pro diffractometer with Cu-K α radiation ($\gamma = 1.5478 \text{ \AA}$). The ^1H NMR spectrum was collected using a 400 MHz Varian INOVA spectrometer and was referenced to the residual solvent peak. To obtain the crystallographic data, UPC-121 and UPC-122 were taken from the mother liquid without further treatment. They were transferred to an oil environment and mounted onto a loop for single crystal X-ray data collection. All crystals data were collected with a SuperNova diffractometer equipped with mirror Cu-K α radiation ($\lambda = 1.54184 \text{ \AA}$) and an Eos CCD detector. The data was collected with a ω -scan technique and an arbitrary ϕ -angle. Data reductions were performed with the CrysAlisPro package, and an analytical absorption correction was performed. All the structures were solved by the direct method using the SHELXS program of the SHELXTL package and refined by the full-matrix least-squares method with SHELXL.¹

Gas adsorption–desorption measurements of N_2 , C_2H_2 , and C_2H_4 on UPC-121 and UPC-122 were collected on the Micromeritics ASAP 2020. The temperatures of 77 K, 273 K, and 298 K were maintained with a liquid nitrogen bath, an ice-water bath, and under room temperature, respectively. The measurements were carried out at 77 K (N_2), 273 K (C_2H_2 and C_2H_4), 298 K (C_2H_2 and C_2H_4). The BET surface area was calculated using multi-point BET equation with the P/P_0 range of 0.05-0.35. Pore volume was calculated with the maximal adsorption capacity. Pore size distribution was calculated with the non-local density functional theory.

2. Calculation of isosteric heat of adsorption (Q_{st})

Firstly, the virial equation (eqn (1)) was used to fit the gas adsorption isotherms at 273 K and 298 K, and then the obtained parameters were inserted into the formula (eqn (2)) to obtain the isosteric heat of adsorption (Q_{st})

$$\ln P = \ln N + 1/T \sum_{i=0}^m a_i N^i + \sum_{i=0}^n b_i N^i \quad (1)$$

$$Q_{st} = -R \sum_{i=0}^m a_i N^i \quad (2)$$

In the calculation, $m=5$, and $n=2$

3. Calculation of selectivity via ideal adsorption solution theory (IAST)

The gas adsorption isotherms were first fitted to a dual-site Langmuir–Freundlich (DSLFL) model (eqn (3)),

$$q = (q_{sat,A} b_A p^{a_A}) / (1 + b_A p^{a_A}) + (q_{sat,B} b_B p^{a_B}) / (1 + b_B p^{a_B}) \quad (3)$$

where q is the amount of adsorbed gas (mmol g^{-1}), P is the bulk gas phase pressure (atm), q_{sat} is the saturation amount (mmol g^{-1}), b is the Langmuir–Freundlich parameter ($\text{atm}^{-\alpha}$), and α is the Langmuir–Freundlich exponent (dimensionless) for two adsorption sites A and B indicating the presence of weak and strong adsorption sites.

IAST starts from the Raoult's Law type of relationship between the fluid and adsorbed phase,

$$P_i = P y_i = P_0 i x_i \quad (4)$$

$$\sum_{i=1}^n x_i = \sum_{i=1}^n P_i / P_0 \quad (5)$$

where P_i is the partial pressure of component i (atm), P is the total pressure (atm), and y_i and x_i represent mole fractions of component i in gas and the adsorbed phase (dimensionless). $P_0 i$ is the equilibrium vapour pressure (atm).

In IAST, $P_0 i$ is defined by relating to spreading pressure π ,

$$\pi S / RT = \int P_0 i q_i(P_i) / P_i dP_i = \Pi(\text{constant}) \quad (6)$$

where π is the spreading pressure, S is the specific surface area of the adsorbent ($\text{m}^2 \text{g}^{-1}$), R is the gas constant ($8.314 \text{ J K}^{-1} \text{ mol}^{-1}$), T is the temperature (K), and $q_i(P_i)$ is the single component equilibrium obtained from isotherms (mmol g^{-1}).

For a DSLFL model, we have an analytical expression for the integral,

$$\int P_0 i q_i(P_i) / P_i dP_i = \Pi(\text{constant}) = q_{sat,A} / \alpha_A \ln [1 + b_A (P_0 i)^{\alpha_A}] + q_{sat,B} / \alpha_B \ln [1 + b_B (P_0 i)^{\alpha_B}] \quad (7)$$

The isotherm parameters are derived from the previous fitting. For a binary component system the unknowns will be Π , $P_0 1$, and $P_0 2$ which can be obtained by simultaneously solving eqn (5) and (7).

The adsorbed amount of each compound in a mixture is

$$q_{mix} = x_i q_t \quad (8)$$

$$1/q_T = \sum_{i=1}^n x_i / q_i(P_0 i) \quad (9)$$

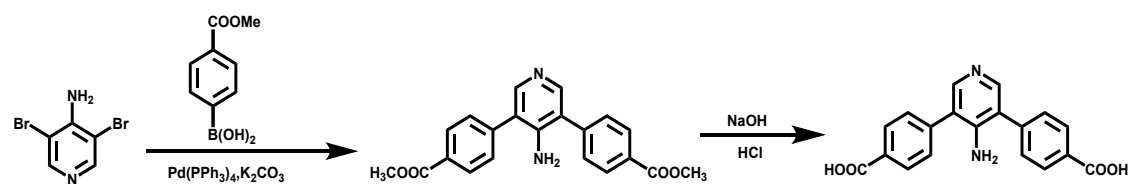
where q_{mix} is the adsorbed amount of component i (mmol g^{-1}), and q_T is the total adsorbed amount (mmol g^{-1}).

The adsorption selectivities S_{ads} were calculated using eqn (10).

$$S_{ads} = (q_1/q_2) / (P_1/P_2) \quad (10)$$

In this study, IAST calculations were carried out assuming a binary mixed gas with a molar ratio of 50:50, 10:90 and 1:99 at 298 K and pressures up to 1 atm.^{2, 3}

4. Synthesis of Ligands



Scheme S1. Synthetic procedures of the H₂APDA ligand.

Synthesis of H₂APDA:

(1) Dimethyl 4,4'-(4-aminopyridine-3,5-diyl)dibenzoate

4-amino-3,5-dibromopyridine (1.26 g, 5.00 mmol), 4-methoxycarbonyl phenylboronic acid (2.16 g, 12.00 mmol), Pd(PPh₃)₄ (0.29 g, 0.25 mmol) and K₂CO₃ (3.32 g, 24.00 mmol) were placed in a 500 mL two-necked round bottom flask under a N₂ gas atmosphere. The flask was further charged with a 200 mL of dry 1,4-dioxane, and the contents were heated for 48 h. After the mixture was cooled to room temperature, the solvent was removed, water was added. The water phase was washed with CH₂Cl₂. After the solvent was removed, the crude product was purified by column chromatography.⁴ ¹H NMR (400 MHz, CDCl₃) 3.96 (s, 6H), 4.39 (s, 2H), 7.57 (d, 4H), 8.17 (s, 2H), 8.20 (d, 4H).

(2) 4,4'-(4-aminopyridine-3,5-diyl)dibenzoic acid

4,4'-(4-aminopyridine-3,5-diyl)dimethyl dibenzoate was dissolved in THF (60 mL), CH₃OH (60 mL) and H₂O (60 mL), then 50 mL 2 M NaOH aqueous solution was added. The mixture was stirred at 60 °C overnight. The organic phase was removed, the aqueous phase was acidified (pH=2~3) with diluted hydrochloric acid to give white precipitate, which was filtered and washed with water several times. ¹H NMR (400 MHz, DMSO-d₆) 7.34 (s, 2H), 7.64 (d, 4H), 8.09 (d, 4H), 8.24 (s, 2H), 13.10 (s, 2H).

5. Synthesis of MOFs

Synthesis of UPC-121

H₂APDA (5.0 mg, 0.025 mmol) and MnCl₂·4H₂O (14.4 mg, 0.0728 mmol) in 3 mL of DMA:C₂H₅OH:H₂O (5:2:1) were ultrasonically dissolved in a Pyrex vial. The mixture was heated in an oven at 100 °C for 24 h. After cooling down to room temperature, dark brown crystals were collected by filtration.

Synthesis of UPC-122

H₂APDA (5.0 mg, 0.025 mmol) and Ni(NO₃)₂·6H₂O (44.8 mg, 0.154 mmol) in 3 mL of DMA:C₂H₅OH:H₂O(5:2:1) were ultrasonically dissolved in a Pyrex vial. The mixture was heated in an oven at 100 °C for 24 h. After cooling down to room temperature, green flake crystals were collected by filtration.

6. Single crystal X-ray Crystallography

Table S1. Crystal data and structure refinement for UPC-121 and UPC-122.

Compound	UPC-121	UPC-122
CCDC	2141833	2141832
Formula	C _{9.5} H ₆ Mn _{0.5} NO _{1.83}	C ₃₈ H ₃₃ N ₄ Ni ₃ O ₁₃
Formula weight(g/mol)	190.96	929.81
Temperature/K	294.9(4)	150.01(10)
Crystal system	hexagonal	trigonal
Space group	P-62c	R3
<i>a</i> / Å	13.1365	23.5121
<i>b</i> / Å	13.1365	23.5121
<i>c</i> / Å	17.7462	38.3738
α / deg	90	90
β / deg	90	90
γ / deg	120	120
<i>V</i> / Å ³	2652.1	18371.7
<i>Z</i>	12	9
μ /mm ⁻¹	6.284	1.095
<i>F</i> (000)	1166.0	4293.0
Radiation	Cu K α (λ = 1.54184 Å)	Cu K α (λ = 1.54184 Å)
GOF on F ²	1.043	0.921
Reflections collected	6261	15185
R _{int}	0.0479	0.0468
Data	1647	9324
Restraints	6	94
parameters	127	524
R1 [I > 2 σ (I)]	0.0741	0.0654
wR2 [I > 2 σ (I)]	0.2064	0.1623
R1 (all data)	0.0893	0.0950
wR2 (all data)	0.2258	0.1850

Table S2. Bond Lengths for UPC-121.

Atom	Atom	Length/Å
Mn1	O1	2.196(6)
Mn1	O1 ¹	2.196(6)
Mn1	O2 ²	2.248(9)
Mn1	O2 ³	2.248(9)
Mn1	N1 ⁴	2.188(4)
Mn1	O3	2.042(2)

Table S3. Bond Lengths for UPC-122.

Atom	Atom	Length/Å
Ni1	O2 ¹	2.145(3)
Ni1	O3 ²	1.988(3)
Ni1	O8	1.951(4)
Ni1	O9	2.062(4)
Ni1	O11	1.985(3)
Ni1	N14 ¹	2.096(4)
Ni2	O1 ³	1.952(3)
Ni2	O2 ¹	2.219(4)
Ni2	N5	2.107(4)
Ni2	O6	1.992(3)
Ni2	O11	2.017(3)
Ni2	O19	2.027(4)
Ni3	O5	2.122(4)
Ni3	O9	2.061(4)
Ni3	O4 ²	2.036(3)
Ni3	O0AA	1.994(3)

7. Powder X-ray Diffraction

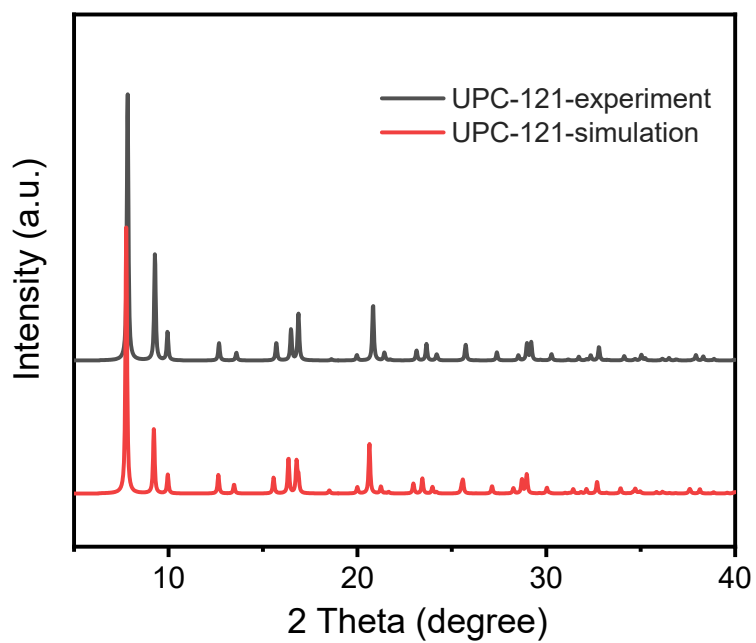


Figure S1. The PXRD patterns of UPC-121.

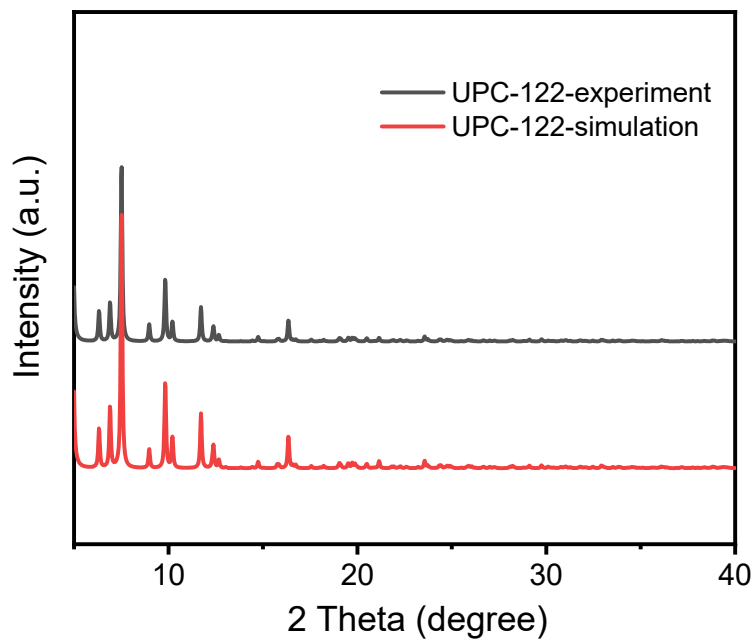


Figure S2. The PXRD patterns of UPC-122.

8. ^1H -NMR spectral data

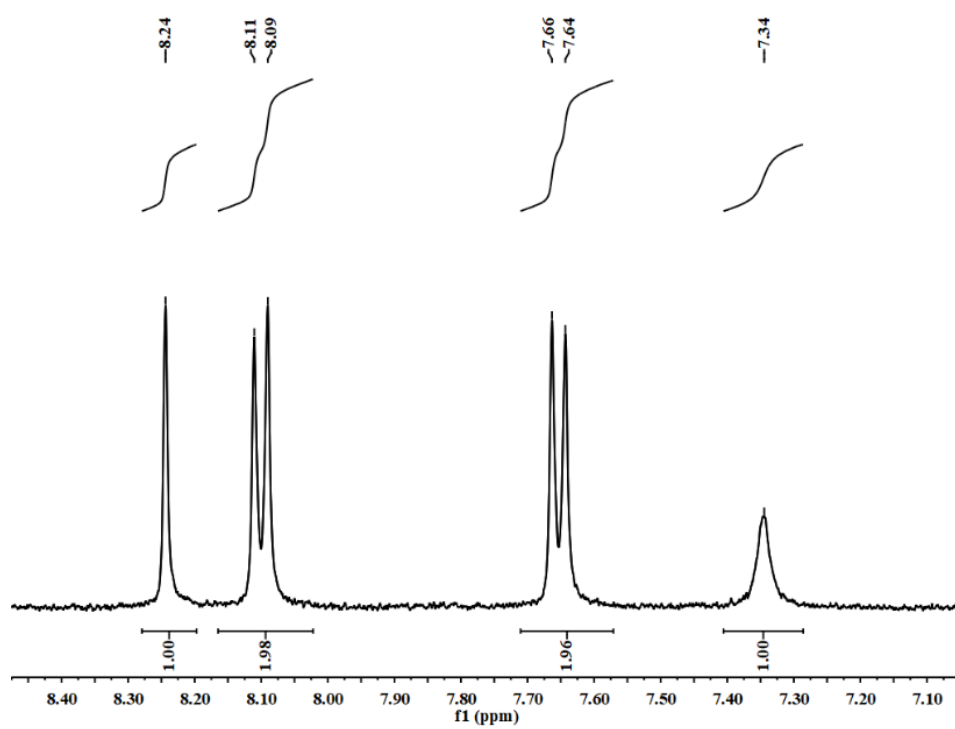


Figure S3. ^1H -NMR spectrum of Ligand H_2APDA .

9. Thermogravimetric Analysis

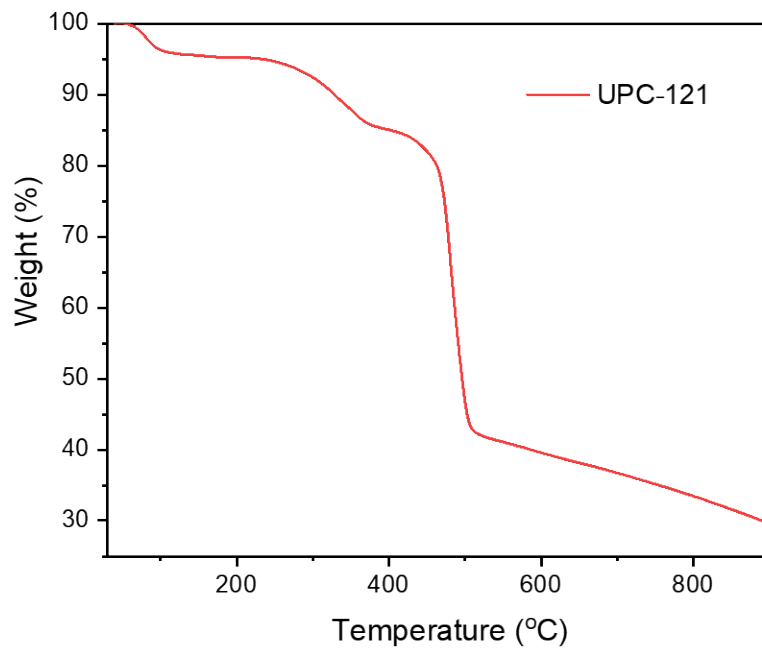


Figure S4. The TGA curves of UPC-121.

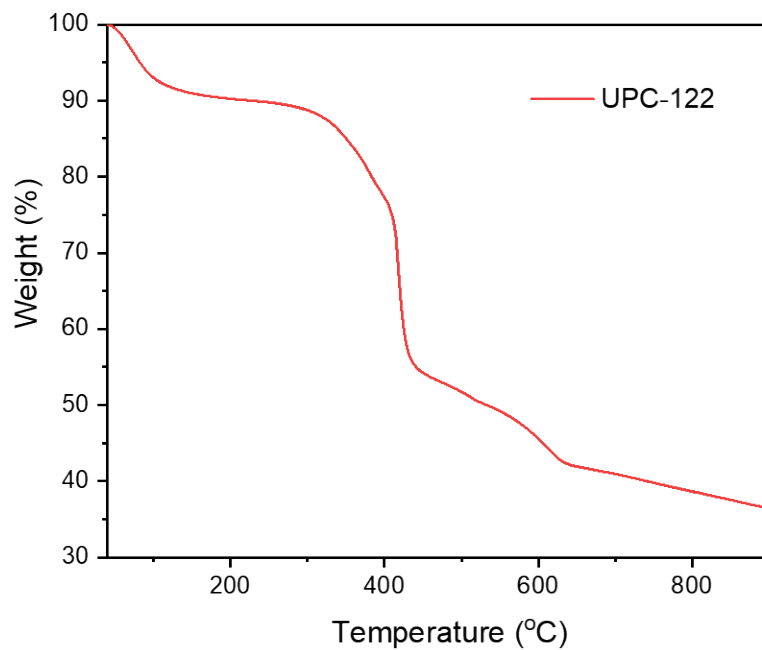


Figure S5. The TGA curves of UPC-122.

10. IR spectrum

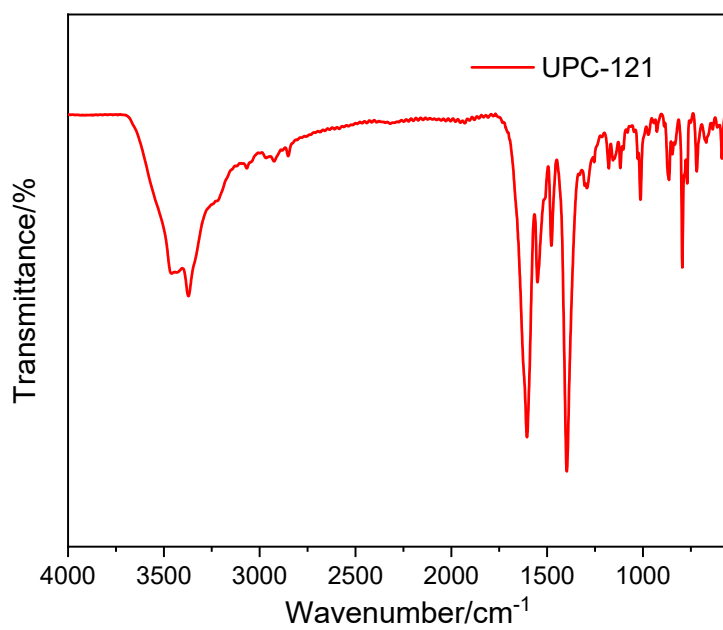


Figure S6. FT-IR spectrum of UPC-121.

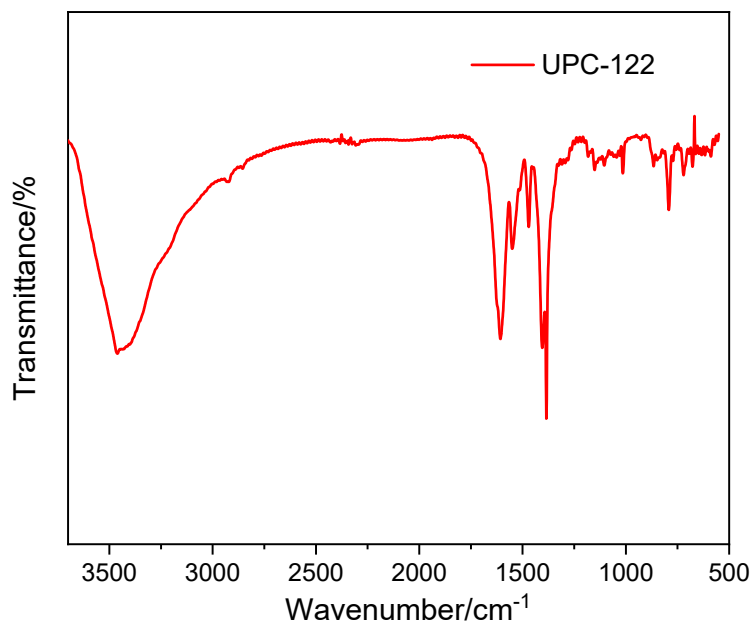


Figure S7. FT-IR spectrum of UPC-122.

11. SEM images

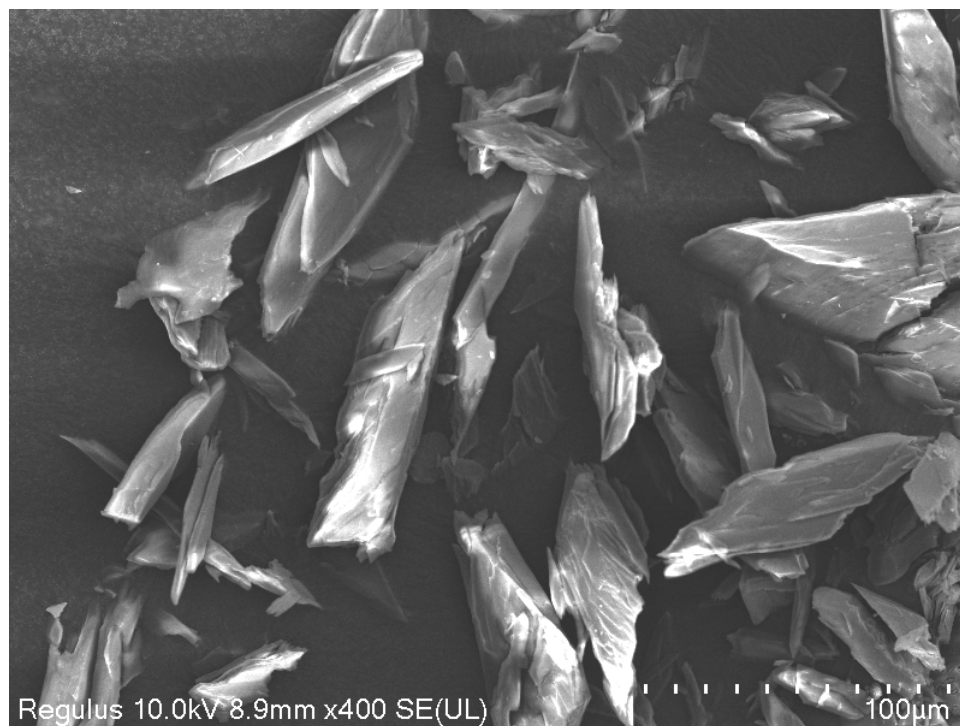


Figure S8. SEM image of UPC-121.

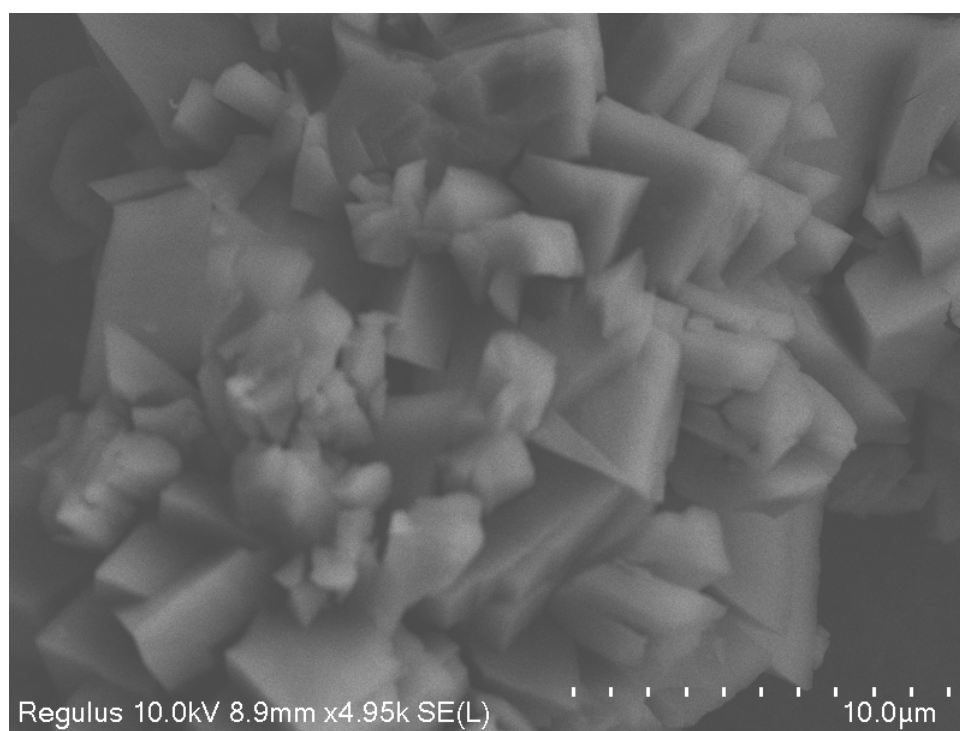


Figure S9. SEM image of UPC-122.

12. Structure diagram of UPC-122

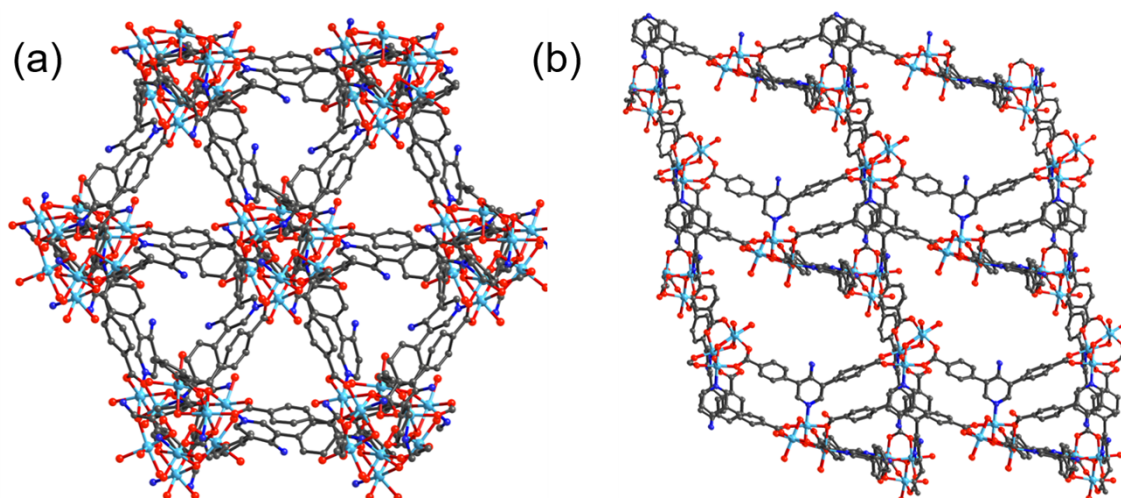


Figure S10. (a) Structure diagram of UPC-122 along C-axis; (b) A three-dimension diagram of UPC-122.

13. Adsorption isotherms of UPC-122 at 273 K

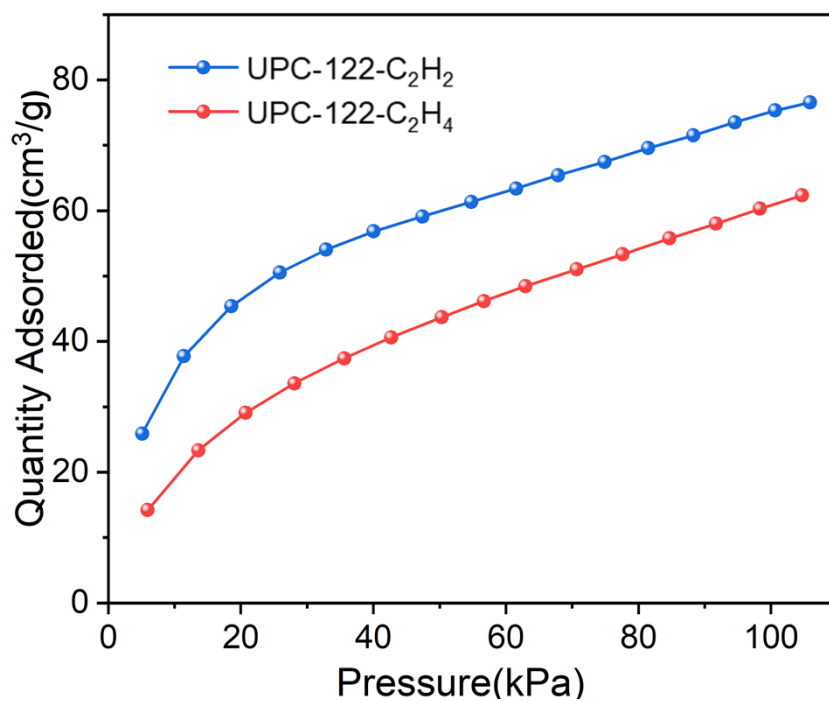


Figure S11. Adsorption isotherms of UPC-122 at 273 K.

14. Adsorption sites simulation based on GCMC

The Grand Canonical Monte Carlo (GCMC) calculations, performed by SORPTION code embedded in the Material Studio software, were carried out to study the C₂H₂/C₂H₄ adsorption capacity of UPC-122 at given adsorption 298 K and 1 atm pressure. The atomic locations were derived from the experimental crystal data. In view of the size of the task to complete the calculations using a whole MOF unit cell, the MOF framework is not geometrically optimized. Periodic boundary conditions were applied in three dimensions. The favorable adsorption sites were simulated by the locates task. In the simulations, we have modeled the framework and gas molecule as rigid and the universal force field (UFF) was applied. Specifically, the van der Waals interactions with a cutoff of 18.5 Å were depicted by the Lennard-Jones potential.

15. References

1. Y. Wang, L. Feng, W. Fan, K. Y. Wang, X. Wang, X. Wang, K. Zhang, X. Zhang, F. Dai, D. Sun and H.-C. Zhou, *J. Am. Chem. Soc.*, 2019, **141**, 6967–6975.
2. W. Fan, S. Yuan, W. Wang, L. Feng, X. Liu, X. Zhang, X. Wang, Z. Kang, F. Dai, D. Yuan, D. Sun and H.-C. Zhou, *J. Am. Chem. Soc.*, 2020, **142**, 8728–8737.
3. Y. Wang, C. Hao, W. Fan, M. Fu, X. Wang, Z. Wang, L. Zhu, Y. Li, X. Lu, F. Dai, Z. Kang, R. Wang, W. Guo, S. Hu and D. Sun, *Angew. Chem. Int. Ed. Engl.*, 2021, **60**, 11350–11358.
4. N. Xu, Q. Zhang, B. Hou, Q. Cheng and G. Zhang, *Inorg Chem*, 2018, **57**, 13330–13340.